



Rod-shaped ZnO nanoparticles: synthesis, comparison and in vitro evaluation of their apoptotic activity in lung cancer cells

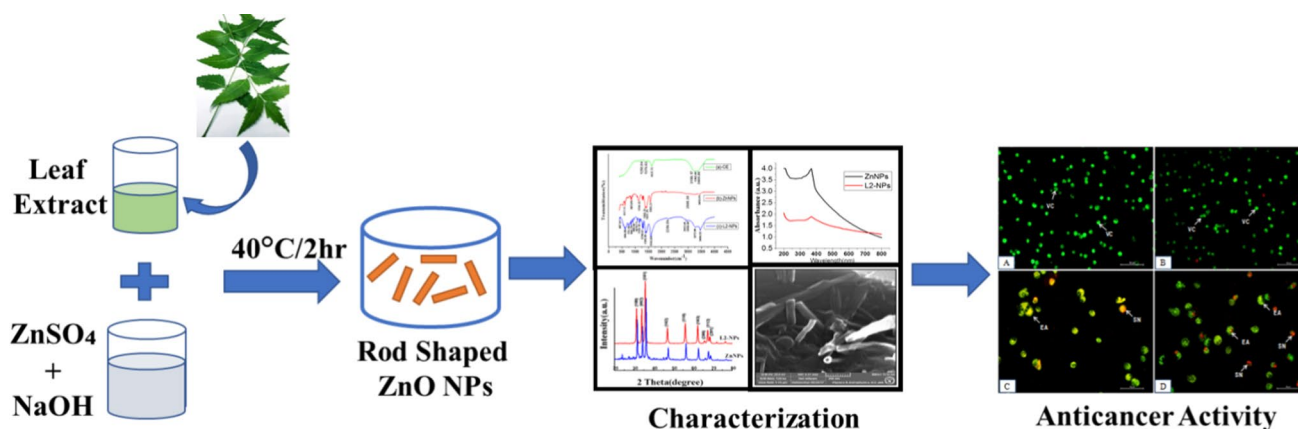
Nutan Rani¹ · Kavita Rawat² · Mona Saini¹ · Anju Shrivastava² · Ganeshlenin Kandasamy³ · Kalawati Saini¹ · Dipak Maity⁴

Received: 30 July 2021 / Accepted: 13 October 2021 / Published online: 22 October 2021
© Institute of Chemistry, Slovak Academy of Sciences 2021

Abstract

Here, we present the synthesis of rod-shaped zinc oxide (ZnO) nanoparticles (NPs) through the wet-chemical method and green synthesis method (using *Azadirachta indica* leaf extract). Physicochemical properties of the ZnO NPs are characterized using different techniques, and their rod shape structure is confirmed via scanning electron microscope (SEM). Biological effects of the rod-shaped ZnO NPs in human lung (A549) cancer cells are evaluated, which include: viability, apoptosis/cell death, and morphological impact. It has been observed that ZnO NPs synthesized via the green method (marked as L2-NPs) have significantly decreased viability of A549 cells, as compared to NPs synthesized via the wet-chemical method (marked as ZnNPs), ascribed to the presence of therapeutic biomolecules (including polyphenols) in leaf extracts as capping agents. It has also been witnessed that the viability of A549 cells can be significantly reduced in a dose-dependent manner with L2-NPs as well as with only extract of leaf of *Azadirachta indica*, an IC₅₀ value of 130.95 µg/mL is obtained. Treatment of A549 cells via L2-NPs has effectively (i) improved apoptotic induction post-incubation and (ii) arrested cell cycles in different phases, where a high cell cycle arrest percentage of 83.1% is obtained in the G1-phase itself. Thus, rod-shaped ZnO NPs synthesized via *Azadirachta indica* leaf extracts have proven to be a potential therapeutic candidate for lung cancer treatment.

Graphic abstract



Keywords Rod-shaped ZnO nanoparticles · *Azadirachta indica* · A549 cells · Apoptosis · Cancer treatment

✉ Kalawati Saini
kalawati.saini@mirandahouse.ac.in

✉ Dipak Maity
dipakmaity@gmail.com

Extended author information available on the last page of the article

Introduction

Globally, cancer (a stage of uncontrolled cell proliferation) is considered the second leading cause of human death. During the past few decades, chemotherapy has been used widely

to treat cancer cells, where toxic anticancer drugs such as alkylating agents, antimetabolites, and so on are involved. One major problem associated with chemotherapy is that the inability of these anticancer drugs to effectively differentiate between cancerous cells and normal cells and treat them consecutively. Recently in current cancer biomedical research, there is a growing demand for the use of nanoparticles for the treatment of cancer cells (Wang and Thanou 2010). Among different nanoparticles, zinc oxide nanoparticles (ZnO NPs) are utilized in many cancer biomedical applications such as drug delivery, bioimaging, and therapeutics as they can induce selective killing of the tumor cells (Martínez-Carmona et al. 2018; Xiong 2013; Mishra et al. 2017). For instance, it has been demonstrated that the ZnO NPs can induce the increased activity of caspase-3 enzyme, DNA fragmentation, and also oxidative stress production during the treatment of HepG2 cancer cells, whereas no risks have been posed to normal rat cells (astrocytes and hepatocytes) (Akhtar et al. 2012). In another investigation, Rasmussen et al. have reported the utilization of ZnO NPs for selective and effective destruction of the tumor cells (Rasmussen et al. 2010). It has been proven that the extent of cell death (apoptosis) in HepG2 and MCF-7 cancer cell lines can be increased by incrementing the therapeutic concentrations of the ZnO NPs (Wahab et al. 2014). ZnO NPs can also increase reactive oxygen species (ROS) generation to induce cell death in cancer cells such as LTP-a-2 cells (Wang et al. 2015) and glioma cells (Ostrovsky et al. 2009).

Apart from the above, ZnO NPs can be combined with other nanoparticles for enhancing cancer treatments. Lately, the ternary nanocomposites of ZnO combined with reduced graphene oxide (r-GO) and stannic oxide (SnO_2) have improved the anticancer application via oxidative stress pathways (Ahamed et al. 2021; Tanino et al. 2020). ZnO and ceria NPs have been synthesized and are compared based on reactive oxygen species (ROS)-mediated cytotoxic activity on MG-63 human osteosarcoma cell lines (Sisubalan et al. 2017), where ZnO NPs are found to be more effective. In addition, deep investigations have been done to determine the effect of size and dispersion status of ZnO NPs toward cytotoxicity and genotoxicity on human bronchial epithelial cells (Roszak et al. 2016).

Moreover, ZnO NPs prepared via the green synthesis process using biological extracts tend to have more therapeutic effects as compared to a chemical method based on ZnO NPs. For instance, ZnO NPs that are green synthesized using rutin (a bioflavonoid) have produced improved antioxidant, antibacterial, and also anticancer/cytotoxic effects (Bharathi and Bhuvaneshwari 2019; Suresh et al. 2018; Selim et al. 2020a; Hanley et al. 2008; Guo et al. 2008; Ryter et al. 2007). Usually, the photodynamic nature of the ZnO NPs is responsible for the anticancer activity, as it can induce ROS and results in cancer cell apoptosis

(Li et al. 2010). In a recent article, photodynamic effects along with the amount of ROS generation and oxidative damages have been investigated against the size-dependent ZnO NPs, where it has been found that the higher intracellular release of zinc ions resulted in enhanced cancer cell death via mitochondrial-mediated apoptosis (Song et al. 2010; Sharma et al. 2012; Stowe and Camara 2009). Besides, the green synthesized ZnO NPs (using the extracts of leaves and stem of *Hyssopus officinalis*, and so on) tend to improve the cancer cell apoptosis in both in vitro and in vivo environments in different cancer cells including liver and bone cancer cells (Rahimi Kalateh Shah Mohammad et al. 2019, 2020; Govarthan et al. 2020; Haitao et al. 2020; Salari et al. 2020; Selim et al. 2020b; Cheng et al. 2020; Sukri et al. 2019; Rauf et al. 2019). However, so far there are no studies that compare the effects of ZnO NPs (especially rod-shaped), which are synthesized through chemical and green synthesis methods, on the apoptosis induction process in cancer cells. Hence in this paper, we initially performed the structural characterization of ZnO NPs synthesized via the chemical wet method (marked as ZnNPs) and via 2 mL extract of *Azadirachta indica* leaves (marked as L2-NPs), and compared their physicochemical properties. Then, we have investigated in detail their apoptosis induction capacity on lung cancer cell lines (A549) using assays like MTT assay, crystal violet assay, and flow cytometry.

Materials and methods

Materials

All chemicals and reagents are analytical reagents (A.R) grade. Pure zinc sulfate heptahydrate ($\text{ZnSO}_4 \cdot 7\text{H}_2\text{O}$) and sodium hydroxide (NaOH) are procured from Central Drug House (P) Ltd – CDH, India. Dulbecco's modified Eagle's medium (DMEM) and (3-(4,5-dimethylthiazol-2-yl)-2,5-diphenyltetrazolium bromide) tetrazolium (MTT) are purchased from Sigma-Aldrich, USA. Fetal bovine serum (FBS) is acquired from Invitrogen. Dimethyl sulpho-oxide (DMSO) and methanol are purchased from SRL, India. Crystal violet, RNase, acridine orange (AO), and propidium iodide (PI) are purchased from Bangalore Genei. A549 cells are obtained from the National Cell Repository of Animal Cells NCCS, Pune, India.

Collection of plant leaves

Healthy and fresh leaves of *Azadirachta indica* are collected from the Department of Chemistry, University of Delhi.

Preparation of 25% of leaf extract

The leaves of *Azadirachta indica* are washed with double distilled water, dried in a hot air oven (for 2 h at 60 °C), and ground to form a powder. Then, 25 g of powder is added in 100 mL of double distilled water and kept on a hot plate magnetic stirrer (at 40 °C for half an hour). This extract is later filtered through Whatman filter paper and then consecutively used in the green synthesis of ZnO NPs.

Synthesis of ZnO NPs

ZnO NPs are prepared through two methods: (i) the green method and (ii) the wet-chemical method. In the green method, an aqueous solution (50 mL) of pure zinc sulfate heptahydrate ($\text{ZnSO}_4 \cdot 7\text{H}_2\text{O}$) at a concentration of 0.2 M is taken as a source of zinc metal ion in a beaker. Then, the aqueous solution (50 mL) of 1 M sodium hydroxide (NaOH) and 2 mL of priorly-prepared leaf extract of *Azadirachta Indica* is poured into the beaker containing zinc precursor solution. Similarly in the wet-chemical method, the amounts of reaction precursors are taken as follows: 0.2 M of $\text{ZnSO}_4 \cdot 7\text{H}_2\text{O}$ + 200 mM tri-sodium citrate (TSC) + 1 g NaOH in 100 mL of solution, herein TSC is used as a capping agent. Both reaction setups are kept on a hot plate with magnetic stirring at 350 rpm at a temperature of 40 °C (313 K). The as-synthesized ZnO NPs via the green method and wet-chemical method are centrifuged, washed with 90% alcohol, dried at 60 °C in a hot air oven, and then stored (in both suspension and dried forms). All the NPs preparations are made using double distilled water. Herein, ZnO NPs synthesized via the green method and wet-chemical methods are named as L2-NPs and ZnNPs, respectively.

Characterization of ZnO NPs

UV–Visible absorption spectra have been recorded using Epoch™ Microplate Spectrophotometer (BIO-TEK®, USA). We have dispersed 20 mg of dry powder of green synthesized ZnO NPs (L2-NPs) in 2 mL deionized water using an ultrabath (sonicator). Herein, deionized water is used as a reference in a cuvette. After that, the test solution (L2-NPs dispersed in deionized water) is filled in a cuvette to measure the UV–Visible absorption spectra. Similarly, the UV–Visible absorption spectrum is recorded for chemical wet synthesized ZnO NPs (ZnNPs). The composition of ZnO NPs is determined via Fourier transform infrared (FTIR) spectroscopy using 55-Spectrometer (Bruker, USA), where KBr is used as the reference material. Moreover, the crystalline nature of the ZnO NPs (dried powder) at room temperature is determined via X-ray

diffraction (XRD) pattern by using D8 Discover X-ray diffractometer, Bruker equipped with Cu K ($\lambda = 1.54056 \text{ \AA}$) as X-ray source, with 2θ value in a range of 20°–80° and 0.0194 degree/sec increments. Surface morphology and topography of ZnO NPs (L2-NPs/ZnNPs) are evaluated by using a field emission scanning electron microscope (FE-SEM, JSM-7600F, JEOL Inc, Japan) and scanning electron microscope (SEM, JSM-6610LV, JEOL Inc, Japan) at 20 kV accelerating voltage and 20–120 kX magnification (with a resolution of 3 nm with High Vacuum mode), where the elemental composition is obtained through in-built energy dispersive X-ray spectroscopy (EDS). Moreover, thermal analysis (from RT to 1000 °C) of ZnO NPs is done with thermo-gravimetric analysis using Perking Elmer (model: Pyris diamond TGA/DTA Specifications: Range RT to 1100 °C) TGA/DTA instrument at 10 °C/min increment. Finally, the zeta potential of ZnO NPs is determined via the dynamic light scattering (DLS—nanoPartica SZ-100-Z, Horiba) technique.

Cell culture

Human lung adenocarcinoma A549 cells are obtained from NCCS, Pune and cultured in DMEM medium (Sigma-Aldrich, St. Louis, MO, USA) with heat-inactivated fetal bovine serum (10% (v/v)). All cultures are maintained in a humidified atmosphere under 5% CO_2 at 37 °C. The cells have been passaged once every 2 to 3 days, taking the logarithmic growth phase of the A549 cells for various experiments (MTT assay, Crystal violet assay, and Flow Cytometry).

MTT assay

To ascertain the viability of A549 cells, an MTT assay is performed. 5×10^4 cells/well are plated in a 96 well plate and incubated in DMEM overnight to acclimatize at 37 °C and 5% CO_2 . The cells are then treated with different concentrations (i.e., 100, 150, 200, and 250 $\mu\text{g/mL}$) of ZnO NPs and further incubated for 24 and 48 h in a CO_2 incubator at 37 °C. Four hours before termination, culture media is removed and replaced with 180 μL of fresh medium and 20 μL of the MTT solution (5 mg/mL in PBS). Then the plate is incubated for the remaining 4 h in a dark humidified atmosphere at 37 °C in the CO_2 incubator. After incubation, media is removed, and 100 μL of DMSO is added to each well to dissolve the formazan (reduced tetrazolium) crystals formed. The optical density is measured at 570 nm using an Epoch™ Microplate Spectrophotometer (BIO-TEK®, USA). The 50% inhibitory concentration (IC_{50}) is determined by the linear regression from the dose–response curve. Moreover, the percentage of cell viability is calculated as follows:

Percent cell viability

$$= (\text{OD value of treated sample} / \text{OD value of control sample}) * 100$$

Crystal violet assay

To ascertain the change in morphology of A549 cells after incubation with nanoparticles, a crystal violet assay is conducted. The cells are plated in a 6 well plate and left overnight to adhere. The inhibitory concentration (IC_{50}) dose of ZnO NPs (based on the results of the MTT assay) is used to treat the cells throughout the experiments for 48 h. After 48 h, the medium is removed, and the cells are washed three times with phosphate buffer saline (PBS). Cells are then fixed in 100% methanol for 1 min and stained with crystal violet for less than 1 min. The plate is washed three times with tap water and allowed to dry. Stained cells are then observed under a normal inverted microscope (Nikon) at 200 X magnification. The changes in cellular morphology are assessed and compared with the untreated control cell population.

Acridine orange/propidium iodide (AO/PI) staining

The effect of nanoparticles in inducing cell death (apoptosis) in A549 cells is determined using acridine orange (AO) and propidium iodide (PI) double staining. A549 cells are plated in a 6 well plate and incubated overnight to allow attachment. The cells are then exposed to IC_{50} dose of ZnO NPs for 48 h. After incubation, the cells are washed two times with PBS and then trypsinized and centrifuged at 1500 rpm for 3 min. The cells are then resuspended in cold PBS and centrifuged again to obtain fresh clean cell pellets. The obtained fresh pellets are then mixed with an equal volume (1:1) of fluorescent dye staining solution comprising 10 $\mu\text{g}/\text{mL}$ of AO and 10 $\mu\text{g}/\text{mL}$ of PI (dissolved in PBS). The freshly stained cell suspension is dropped onto a clean glass slide and covered with a coverslip for even distribution of cells and then observed under a UV–fluorescence microscope (Nikon) within 30 min, before fading of the fluorescence. The morphological standards used for the classification of viable, apoptotic, and necrotic cells are as follows: (i) viable cells (VC) show a green nucleus with a round intact structure; (ii) early apoptosis displays a dense bright-green nucleus with chromatin condensation (CC) and nuclear blebbing (BL); (iii) late apoptosis (LA) exhibits a dense orange area, and (iv) secondary necrosis (SN) shows an orange/red intact nucleus.

Cell cycle analysis with flow cytometry

Flow cytometry is performed for quantifying DNA content and to analyze different phases of the cell cycle. PI is used

to label the nuclear DNA content. A549 cells are treated with IC_{50} dose of ZnO NPs for 48 h. Briefly, about 1×10^6 cells are harvested and resuspended in PBS. After centrifugation, a fresh pellet is obtained, which is fixed by adding 70% chilled ethanol prepared in PBS. The cells are incubated for 1 h in $-20\text{ }^\circ\text{C}$. After incubation, cells are washed with PBS twice and incubated in a staining solution containing 50 μL of RNase solution (100 $\mu\text{g}/\text{mL}$) and 200 μL of PI (50 $\mu\text{g}/\text{mL}$ PI in PBS). The cells are incubated for 30 min at room temperature in dark with gentle rotation (constant). The cell cycle is analyzed with help of a flow cytometer (BD accuri C6 cytometer).

Statistical analysis

One-way ANOVA followed by Dunnett's multiple comparison tests is applied for the analysis of the results. The $p < 0.05$ has been assigned as statistically significant. Graphpad prism 6 version software is used.

Results and discussions

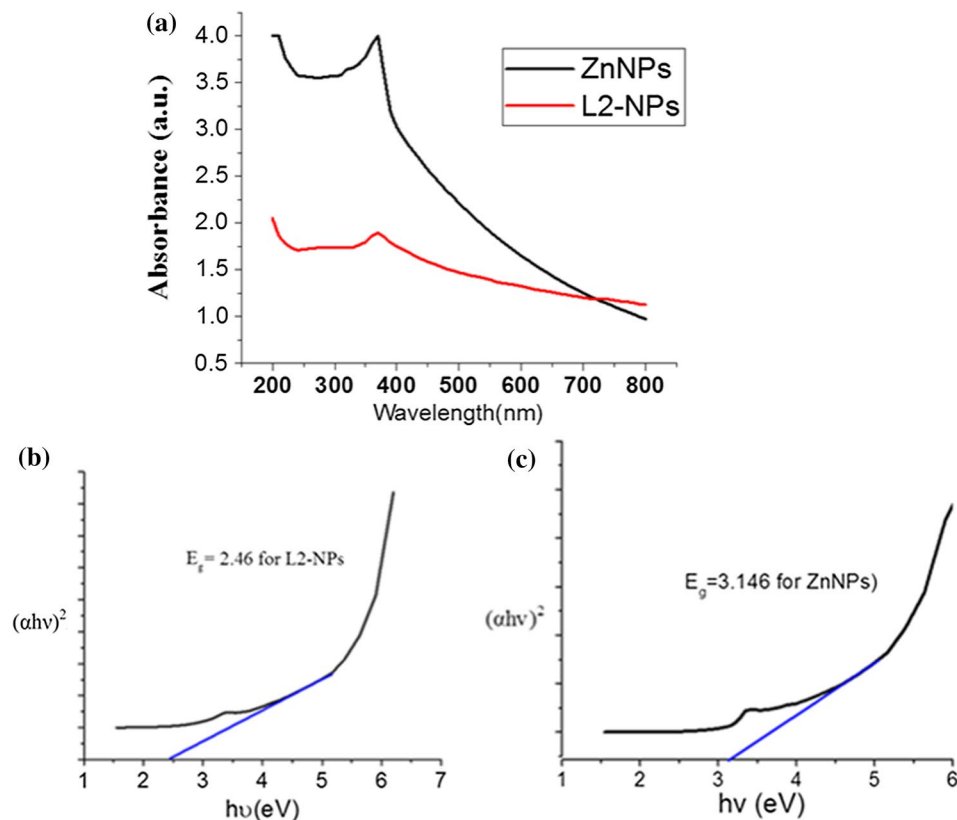
UV–visible spectroscopic analysis

The UV–Visible spectra show a sharp absorption band at 368.43 nm for ZnO NPs synthesized with green method (L2-NPs) and 369.18 nm for ZnO NPs with chemical wet method (ZnNPs), respectively, where these spectra are shown in Fig. 1a, and they are matching with the maximum absorption peak reported at 370 nm for ZnO NPs in the literature (Padalia and Chanda 2017; Jayaseelan et al. 2012). The tauc plots obtained from UV–Visible absorption spectrum data of green synthesized and wet-chemical synthesized ZnO NPs are given in Fig. 1b and c, respectively. The value of the energy bandgap has been evaluated from the following tauc's formula.

$$(\alpha h\nu)^2 = A(h\nu - E_g)^{1/2}$$

where A is the constant which does not depend upon the photon energy, and $h\nu$ is the photon energy. Moreover, the energy bandgap (E_g) has been evaluated via $(\alpha h\nu)^2$ versus $h\nu$ curve as given in tauc plot. It has been noted that the bandgap energies of 2.46 eV and 3.146 eV are, respectively, obtained for L2-NPs and ZnNPs, which match with the reported values (Rani et al. 2020; Khan et al. 2018; Hamrouni et al. 2014). Herein the capping efficiency of tri-sodium citrate (TSC) is higher than the phytochemicals present in leaf extract. Since, quantity of phytochemical present in 2 mL is very less than the 200 mM of tri-sodium citrate which is used in chemical wet synthesis of ZnO NPs.

Fig. 1 **a** UV–Visible absorption Spectra: For ZnO NPs synthesized with green method (L2-NPs) and with wet-chemical method (ZnNPs), **b** Tauc plots of synthesized ZnO NPs with green method ($E_g = 2.46$ eV for L2-NPs), **c** Chemical wet method ($E_g = 3.146$ eV for ZnNPs)



Therefore, the bandgap energy has been found more for ZnO NPs (ZnNPs) synthesized with chemical wet method than the ZnO NPs (L2-NPs) synthesized with green method.

Bandgap tuning of ZnO NPs can be very useful in cancer therapy as it can increase the threshold energy of reactive oxygen species (ROS) generation and oxidative stress in cancer cells through the generation of higher numbers of holes (h^+) and electrons (e^-) on the surface of the NPs (Zhang et al. 2014; Ahamed et al. 2017).

FTIR spectroscopy and powder X-ray diffraction (PXRD) analysis

Fourier transform infrared spectroscopy (FT-IR) studies have been done in the spectral range of 400–4000 cm^{-1} for only extract (OE) of fresh leaves of *Azadirachta indica*, L2-NPs (ZnO NPs synthesized with 2 mL of leaf extract of *Azadirachta indica*), and ZnNPs (ZnO NPs synthesized with wet-chemical method) and shown in Fig. 2a.

Figure 2a shows the FTIR spectra of the OE of fresh leaves which confirms the peaks at 3311.71 cm^{-1} correspond to $-\text{OH}$ or H_2O molecules, the peak at 1637.72 cm^{-1} correspond to aromatic ring stretching, and the peaks at 1246.29 cm^{-1} , 1288.71 cm^{-1} , 1364.41 cm^{-1} , and 1375.01 cm^{-1} correspond to $-\text{C}-\text{H}$ in-plane bending,

respectively. The expanded spectrum of OE from 1380 to 1200 cm^{-1} has been shown in the inset of Fig. 2a for clarity of the peaks in this region.

The presence of a band at 865.89–617.11 cm^{-1} indicates the metal oxide ($-\text{Zn}-\text{O}-$) bond. Moreover, the presence of a peak corresponding to $\text{C}=\text{O}$ carboxylic in FTIR spectra predicts the active role of TSC as a capping and stabilizing agent in the wet-chemical synthesis process. The FTIR spectrum of L2-NPs is given in Fig. 2c. In this spectrum, bands in the range of 407.01 to 844.76 cm^{-1} are due to metal oxide ($-\text{Zn}-\text{O}-$) stretching. Other bands such as 1070.71 cm^{-1} , 1155.10 cm^{-1} , 1296.63–1395.01 cm^{-1} , and 1592.88 cm^{-1} and 3272.80–3456.53 cm^{-1} are corresponding to aromatic $-\text{C}-\text{H}$ bond, $-\text{C}-\text{O}$ bond, aromatic $-\text{C}=\text{C}$, bending vibrations, and stretching vibration of surface H_2O or $-\text{O}-\text{H}$ bond. Above mentioned bands show the presence of phytochemicals such as phenolic, flavonoids, and so on on the surface of L2-NPs, which indicates the active role of leaf extracts as the capping and stabilizing agent during the green synthesis process (Ramesh et al. 2015; Soto-Robles et al. 2019).

The crystal structures of the ZnO NPs (L2-NPs and ZnNPs) are characterized via XRD (D8 diffractometer, Bruker made, $\text{Cu K}\alpha$ radiation with $\lambda = 1.54056 \text{ \AA}$) and shown in Fig. 2b. The space group for ZnO NPs is (P 63 mc). The 2θ peaks at 31.67°, 34.31°, 36.14°, 47.40°, 56.52°, 62.73°, 66.28°, 67.91°, 69.03°, 72.48°, and 76.53° have been

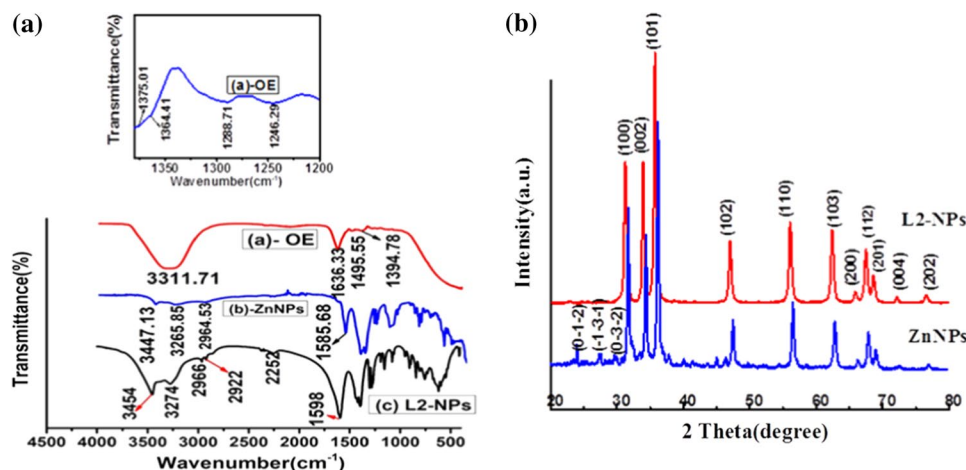


Fig. 2 (A) FTIR Spectra **a** with only extract (OE) leaf of *Azadirachta indica*, **b** ZnO NPs synthesized using chemical wet method (ZnNPs), and **c** ZnO NPs synthesized using green method (L2-NPs), (B) Powder X-ray diffraction pattern of synthesized ZnO NPs—L2-NPs (ZnO NPs synthesized using the green method) and ZnNPs (ZnO NPs synthesized using the wet-chemical method). **b** depicts the FTIR spectra

assigned to (100), (002), (101), (102), (110), (103), (200), (112), (201), (004), and (202) crystal lattices of the ZnO NPs, indicating that the as-synthesized samples (L2-NPs and ZnNPs) have wurtzite crystalline structure. Moreover, the above-mentioned peaks match with the JCPDS No. 36-1451 (Seo and Shin 2015) and with JCPDS 5-0664 (Akhtar et al. 2012). There are three peaks with very small intensities before $2\theta = 30^\circ$. These three additional peaks with small intensities are detected due to presence of the precursor zinc sulfate as impurity which is left over unreacted in chemical wet synthesis. The 2θ peaks at 23.46° , 27.33° , and 30.03° have been assigned corresponding to (hkl) values (012), (131), and (032), respectively. These values match with the reported pattern COD 9,014,256 ($\text{ZnSO}_4 \cdot 4\text{H}_2\text{O}$). It may be due to conversion of precursor $\text{ZnSO}_4 \cdot 7\text{H}_2\text{O}$ into $\text{ZnSO}_4 \cdot 4\text{H}_2\text{O}$ during the chemical synthesis of the ZnO NPs (ZnNPs).

FE-SEM/SEM and TGA analysis

The morphology of the synthesized ZnO NPs has been studied using FE-SEM/SEM. Figure 3a shows the FE-SEM image of the ZnO NPs synthesized with the green method (L2-NPs), where it is clear that the majority of the particles are rod-shaped with smooth surfaces and porous sheet structure. The width of L2-NPs is to be approximately 50–60 nm and length in the range of 200 nm–600 nm. One dimension of the as-synthesized ZnO NPs matches with the reported ZnO NPs prepared using *Cucumis melo inodorus* rough shell extract, where the range of NPs is from 10 nm to 100 nm (Mahdizadeh et al. 2019).

of ZnO NPs obtained from the chemical wet method (ZnNPs), which indicates that the bands at 1583.21 cm^{-1} representing C=O carboxylic acid and the sharper band at 1154.22 cm^{-1} correspond to the presence of C–H group bonds. The peak observed at 2985.35 cm^{-1} is corresponding to C–H stretching

The weight loss in the samples has been determined using thermo-gravimetric analysis. TGA curve of the green synthesized ZnO NPs (L2-NPs) is shown in Fig. 3b. It can be seen that the green synthesized ZnO NPs show 100% mass (M.W.) at 33.50°C . The first % mass loss occurs at $\leq 33.50^\circ \text{C}$ $T \leq 101.56^\circ \text{C}$ due to the presence of absorbed water (H_2O) on the surface of synthesized L2-NPs. Herein, the rate of mass loss is fast, because the rate of evaporation of H_2O is found to be fast. The second stage of % mass loss occurs from 101.56 to 425°C . Herein the rate of decomposition of synthesized L2-NPs is slow as compared to the first stage mass loss %. This step involves two processes, in first process (101.56°C – 196.84°C) the decompositions of phytochemicals takes place by which ZnO NPs (L2-NPs) are capped. In the second step, the degradation of $\text{Zn}(\text{OH})_2$ takes place at around 300°C . After that, again % mass loss is occurring from 425 to 941°C continuously. Similar results are reported by Moharram et al. (Moharram et al. 2014).

The SEM images of ZnO NPs synthesized with the wet-chemical method (ZnNPs) have been given in Fig. 3c and d, where it is clear that the shape of ZnNPs has also been found to be rod and sheet-shaped. There are some NPs with irregular morphology, and the width of ZnNPs is found to be approximately 75–125 nm and length in the range of $0.5 \mu\text{m}$ – $1 \mu\text{m}$.

Figure 4a and b show the TEM images of the ZnO NPs (L2-NPs and ZnNPs) synthesized via green method and wet-chemical method, respectively. It can be seen that both the ZnO NPs have rod/sheet-shaped structure which is also confirmed by the FE-SEM.

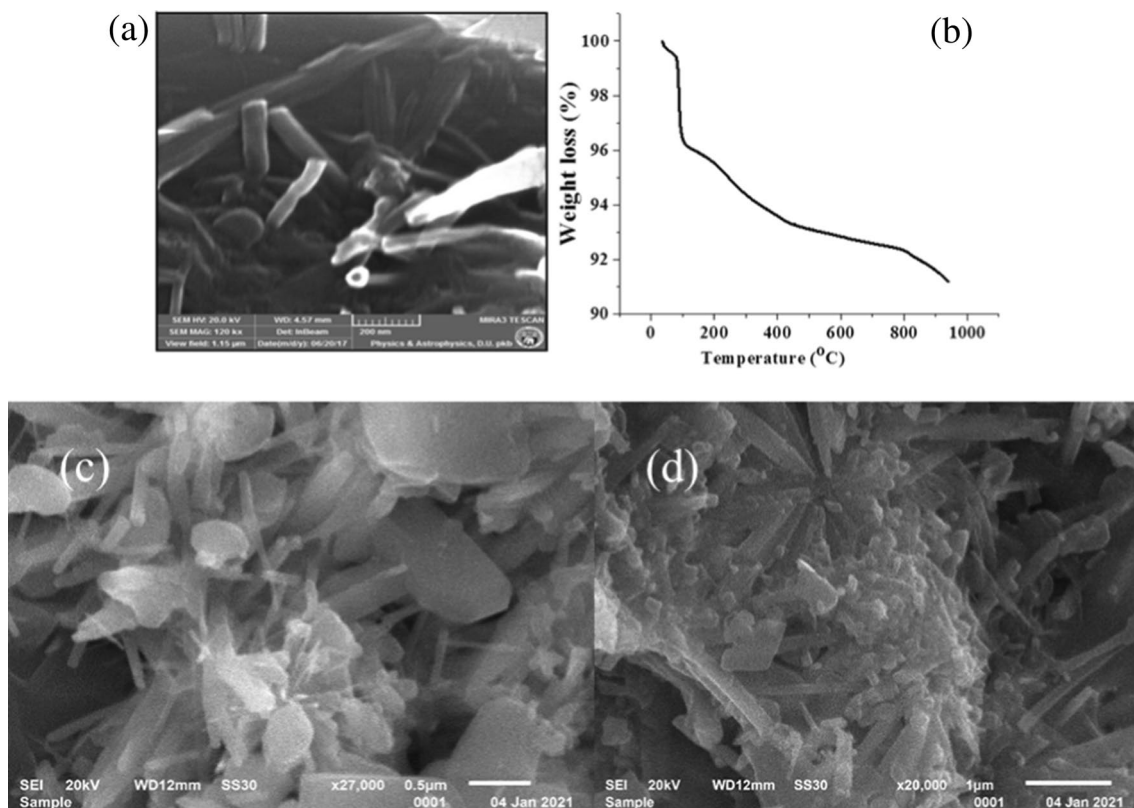
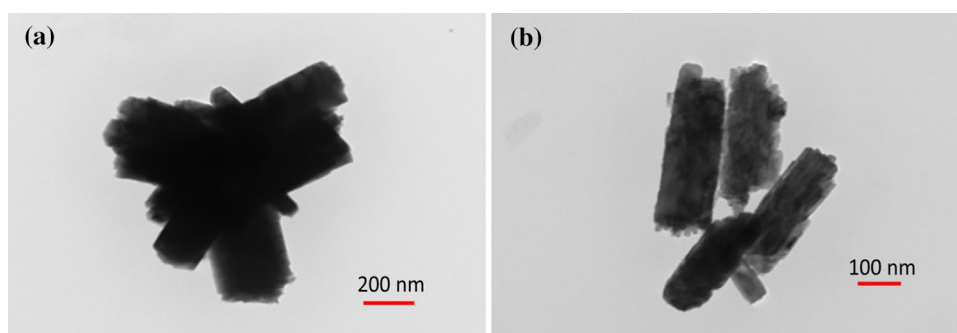


Fig. 3 **a** FE-SEM images of ZnO NPs synthesized with green method (L2-NPs), **b** TGA of ZnO NPs synthesized with green method (L2-NPs), and **c**, **d** SEM images of ZnO NPs synthesized with wet-chemical method (ZnNPs)

Fig. 4 TEM images of **a** green-synthesized ZnO NPs (L2-NPs) and **b** wet-chemical synthesized ZnO NPs (ZnNPs), with magnification at 120 kx



The EDS spectra of L2-NPs and ZnNPs are given in Fig. 5a and b, respectively. The EDS result shows that there are no other elemental impurities present in the as-synthesized L2-NPs and ZnNPs. The elemental compositions of L2-NPs and ZnNPs are given in Tables 1 and 2, respectively. The atomic ratio of L2-NPs is obtained as—51.42% of zinc (Zn) and 48.58% of oxygen (O). The atomic ratio of ZnNPs is obtained as 52.02% of Zn and 47.98% of O. These results are in good agreement with the reported EDS analysis (Rani et al. 2020).

DLS analysis

Agglomeration/stability of NPs in an aqueous state is a major concern in nanomedicine research. From Fig. 6a, b, the zeta potential of ZnO NPs in water medium has been found -28.64 mV for L2-NPs and -34.75 mV for ZnNPs. The above-mentioned zeta potential values show that the as-synthesized L2-NPs and ZnNPs are well-stabilized, which are in good agreement with the reported values by Akhtar et al. and Asik et al. (Akhtar et al. 2012; Mohamed Asik et al. 2019).

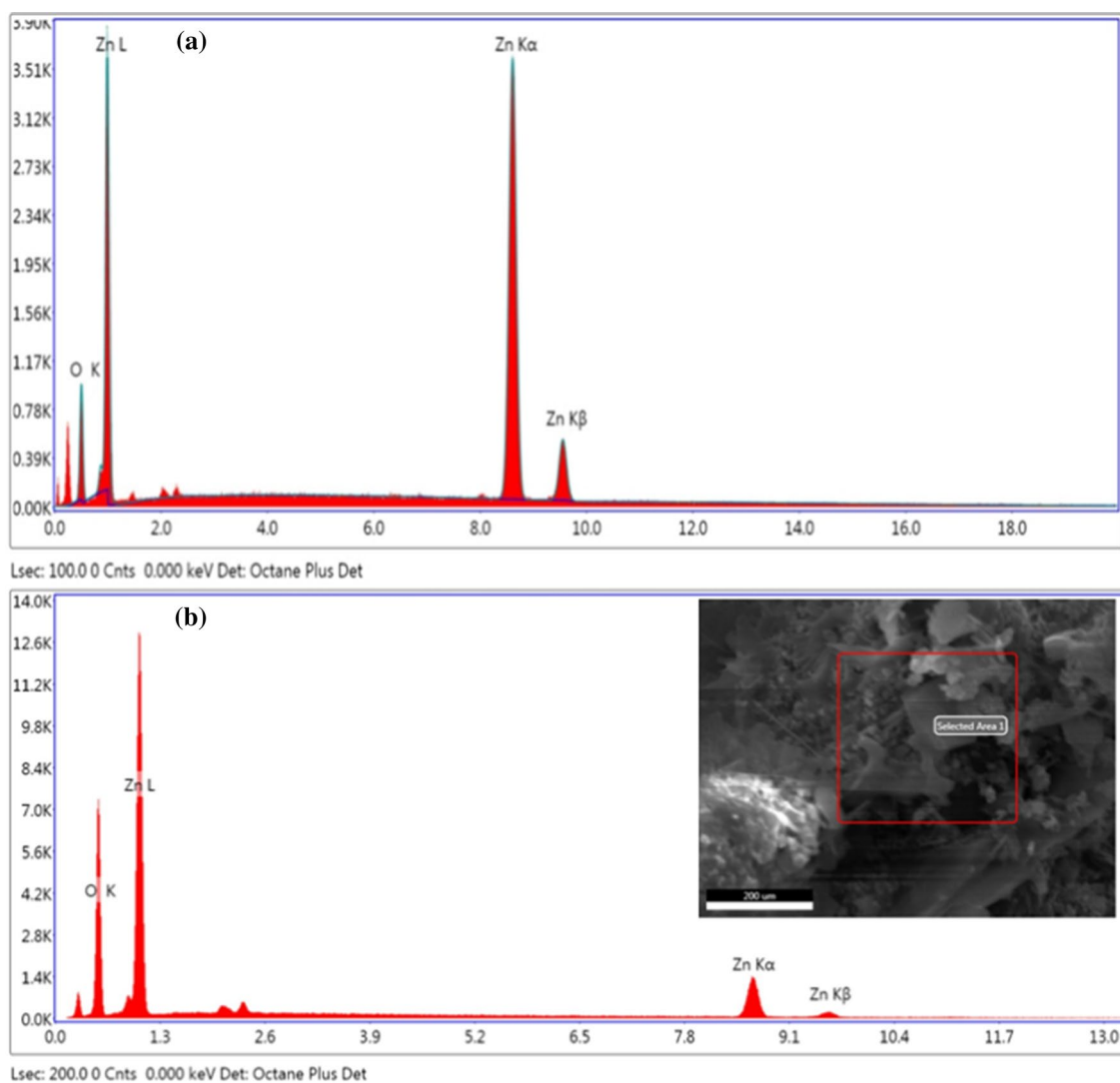


Fig. 5 **a** Energy dispersive spectroscopy (EDS) of synthesized ZnO NPs with green method (L2-NPs) and **b** Energy dispersive spectroscopy (EDS) of synthesized ZnO NPs with chemical wet method

(ZnNPs), where the red square selection indicates that the area under that has been considered for estimating the atomic percentage of the elements present

Table 1 Energy Dispersive Spectroscopy (EDS) analysis for ZnO NPs synthesized with green method (L2-NPs)

Element	Weight %	Atomic %	Net Int	Error %
O K	20.58	51.42	62.76	9.86
Zn K	79.42	48.58	597.00	1.44

Table 2 Energy Dispersive Spectroscopy (EDS) analysis for ZnO NPs synthesized with wet-chemical method (ZnNPs)

Element	Weight %	Atomic %	Net Int	Error %
O K	20.46	47.98	242.76	7.14
Zn K	79.54	52.02	111.71	2.88

Effect of L2-NPs on the viability of A549 cells

The effect of ZnO NPs (L2-NPs and ZnNPs) on the viability of A549 cells is determined by using an MTT assay. This assay is established based on the capability of the NADP(H)-dependent cellular oxidoreductase enzyme to reduce the yellow tetrazolium dye to its insoluble purple formazan, which reflects the proportion of viable cells whereas dead cells do not show this function. Using a microplate reader, the measurement of absorbance at 570 nm (OD value) reflects the number of living cells.

The larger the OD value at 570 nm, the more live cells (refer to Fig. 7a). It should be noted that the ZnO NPs synthesized with the chemical wet method (ZnNPs) did not

Fig. 6 Zeta potential curves of **a** ZnO NPs synthesized with green method (L2-NPs) and **b** ZnO NPs synthesized with the chemical method

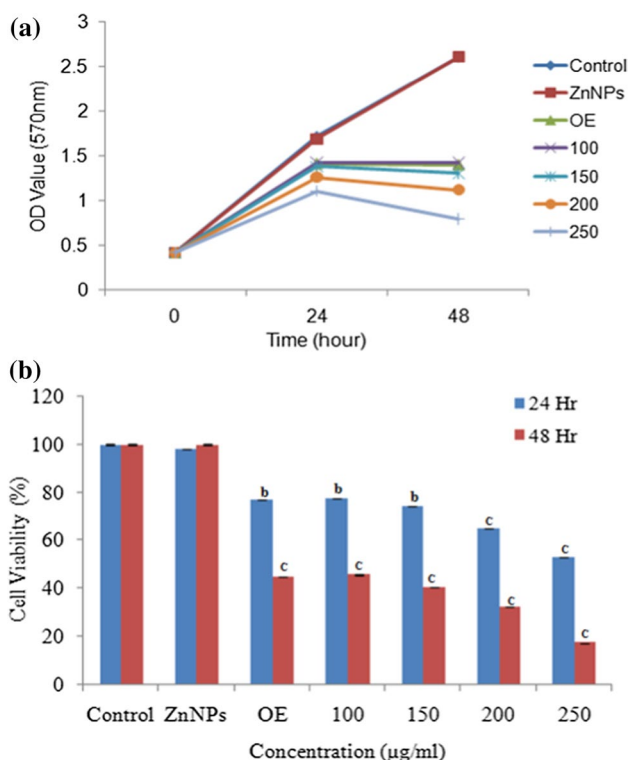
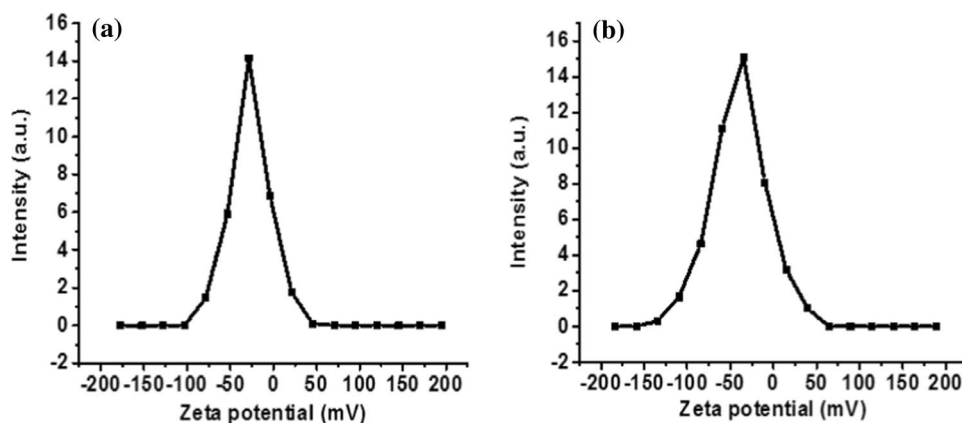


Fig. 7 **a** A549 cells are treated with L2-NPs at the indicated concentrations and time periods. Cell proliferation test is performed using MTT, and absorbance is measured after 24 and 48 h of incubation. Data represent three separate experiments performed in triplicate. **b** Induction of cell death by L2-NPs in A549 cells determined by MTT assay. Cells are treated with different concentrations of L2-NPs (in µg/mL) for 24 and 48 h. Data are represented as mean \pm SD. ($p \leq 0.05^a$, $p \leq 0.01^b$, $p \leq 0.001^c$). Herein, on the x-axis the range of concentration is 100–250 µg/mL for the only extract (OE), ZnNPs (ZnO NPs synthesized with chemical wet method) and L2-NPs (ZnO NPs synthesized with 2 mL of leaf extract of *Azadirachta indica*)

exhibit any cytotoxicity to the cells suggesting that this sample is non-toxic to the cells, and these results match with the reported cell viability values by Prashanth et al. (2015). Moreover, the results depicted in Fig. 7b show that the viability of A549 cells after treating with L2-NPs in

a dose-dependent manner. Herein, it is observed that the cell viability could be significantly reduced with an incubation period of 48 h at 100, 150, 200, and 250 µg/mL. The IC_{50} value for L2-NPs is found to be 130.95 µg/mL after 48 h incubation. The obtained results are similar to the reported works on the usage of ZnO NPs (green synthesized) on MCF-7 cells (Kumar et al. 2006) and HFF cell lines (Rajeshkumar et al. 2018; Umamaheswari et al. 2021; Sharmila et al. 2019; Shilpa et al. 2020; Salari et al. 2019).

Effect of L2-NPs on the morphology of A549 cells

Crystal violet assay is performed to monitor the morphological changes in A549 cells and given in Fig. 8. Cells are stained with crystal violet and imaged at 200 \times magnification in an upright microscope (Nikon). Cells are treated with the IC_{50} dose (130.95 µg/mL) of ZnO NPs synthesized from 2 mL of leaf extracts (i.e., L2-NPs) for 48 h.

We have observed the shrinkage of cells accompanied by rounded cell morphology, poor cell adhesion, and reduced cell number in L2-NPs treated group. Comparatively, there is no significant change in the morphology of A549 cells in the control group and treated with ZnO NPs synthesized with wet-chemical method (ZnNPs). Moreover, the only extract (OE) of leaves of the *Azadirachta indica* treated group has shown slight shrinkage and reduced cell number.

Induction of apoptosis in A549 cells

AO and PI dual staining is performed to study apoptosis. AO stain with green fluorescence penetrates from the plasma membrane of healthy cells or early apoptotic cells with fragmented DNA, whereas PI stain displays dead cells. Specific changes in morphological characterizations of cells such as chromatin condensation, cell shrinkage, nuclear, or cytoplasmic fragmentations indicate the occurrence of apoptosis. A549 cells are treated with IC_{50} dose (130.95 µg/mL) of ZnO NPs (i.e., L2-NPs) and observed under a fluorescent

Fig. 8 Morphology of L2-NPs treated human lung cancer A549 cells. **a** Control group with no treatment, **b** Cells treated with ZnO NPs synthesized with chemical wet method (ZnNPs), **c** Cells treated with the only extract, **d** Cells treated with IC₅₀ dose (130.95 µg/mL) of ZnO NPs synthesized from leaf extract (L2-NPs), magnification-200x

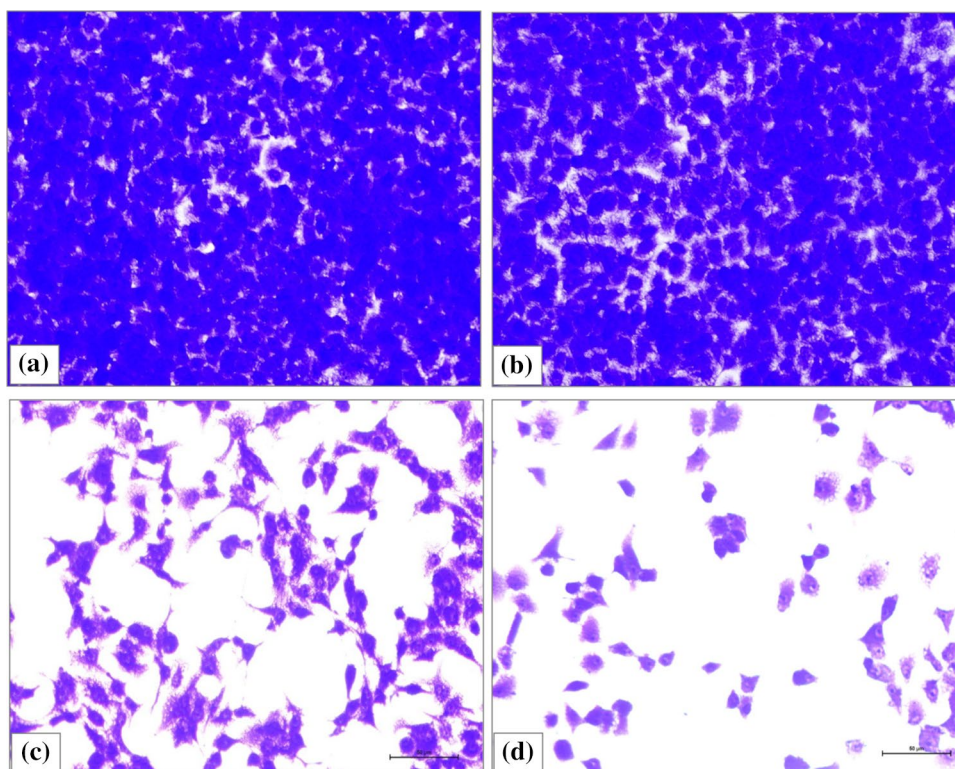
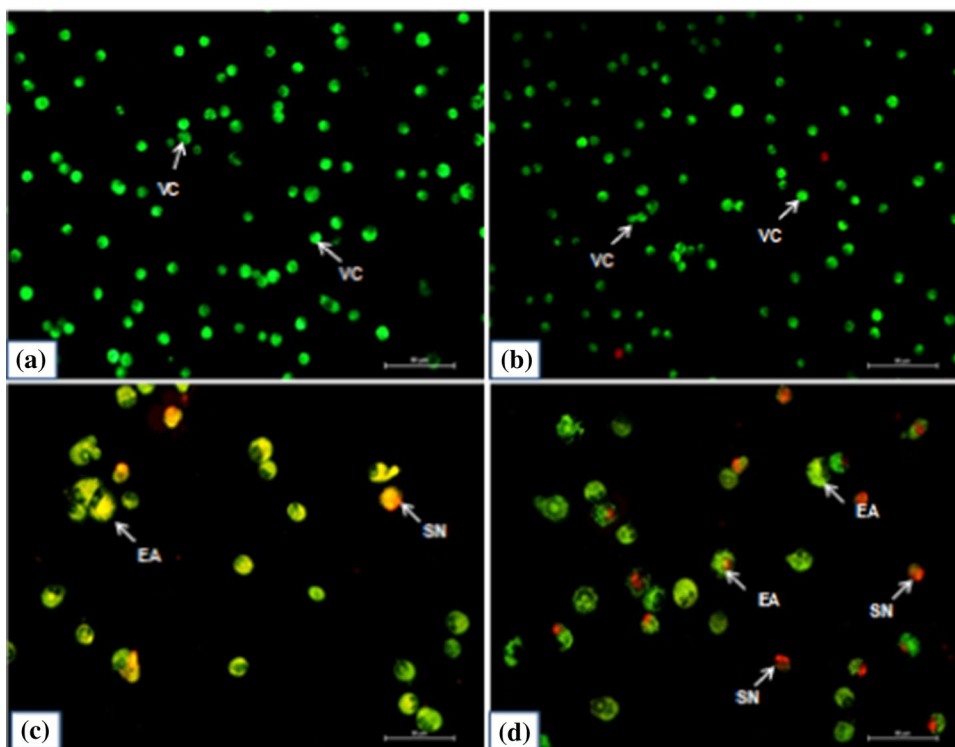


Fig. 9 Morphological and apoptosis analysis of A549 cells double-stained with AO and PI as observed under a fluorescent microscope (Nikon) at 200× magnification. The treated cells were exposed to IC₅₀ dose of L2-NPs (130.95 µg/mL) for 48 h. **a** Untreated cells, **b** Cells treated with ZnO NPs synthesized with chemical wet method (ZnNPs), **c** Cells treated with the only extract, **d** Cells treated with ZnNPs synthesized from leaf extract (L2-NPs). VC: viable cells; EA: early apoptosis; and SN: secondary necrosis



microscope (Nikon) to analyze the viable cells, early apoptosis, and late apoptosis (refer Fig. 9). In our results, A549 cells treated with L2-NPs illustrated some signs of cell death such as chromatin condensation, early apoptosis, and

secondary necrosis. Similar results have been reported with green synthesized ZnO NPs for murine breast tumor model and human breast cancer cell lines (Mahdizadeh et al. 2019).

After 48 h of incubation, untreated A549 cells have shown viable cells (VC) with green color and intact nuclei. In contrast, early apoptosis (EA) and secondary necrosis (SN) is observed in cells treated with IC_{50} dose of L2-NPs. Such type of cytotoxic study is similar to the investigation on ZnO NPs synthesized with *Tabernaemontana divaricata* leaf extract against MCF-7 breast cancer cell lines at various concentrations (6.5–100 $\mu\text{g}/\text{mL}$) (Sivaraj et al. 2014).

Induction of G1 phase cell cycle arrest

We have further analyzed the distribution pattern of the cell cycle by flow cytometry in A549 cells. The effect on cell cycle progression is examined after 48 h exposure to 130.95 $\mu\text{g}/\text{mL}$ of L2-NPs. According to the results displayed in Fig. 10, there is G1 phase arrest in A549 cells after L2-NPs treatment that accounted for 83.1% cells.

In addition, the S and G2 phase cell percentages also dramatically reduced to 8.9% and 4.1%, respectively, in the L2-NPs treated cells. Extract treatment also arrested cell cycle in the G1 phase which accounted for 79.0% of the G1 phase, 10.2% of the S phase, and 8.2% in the G2 phase.

Conclusion

Our results demonstrate the preparation of rod-shaped ZnO NPs using both the green method and the wet-chemical method. In the green method, ZnO NPs (L2-NPs) are synthesized by using a 2 mL fresh aqueous extract of leaves of *Azadirachta indica* (Neem tree). On the other hand, in wet-chemical method, ZnO NPs (ZnNPs) are synthesized by using tri-sodium citrate and sodium hydroxide. The structure/physicochemical properties of the as-synthesized NPs (L2-NPs and ZnNPs) are characterized by different

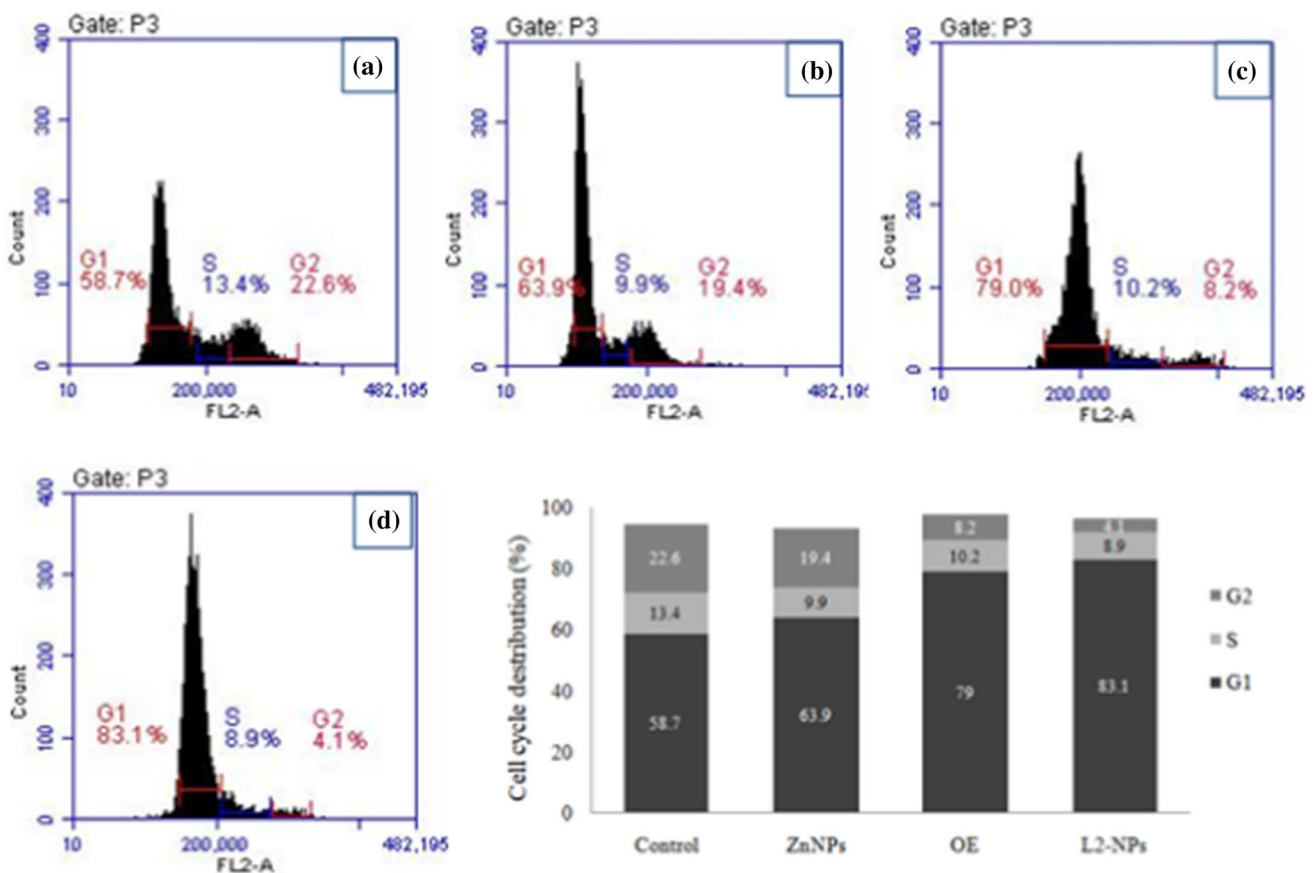


Fig. 10 Flow cytometry analysis of cell cycle arrest in A549 cells treated with 130.95 $\mu\text{g}/\text{mL}$ of L2-NPs for 48 h. **a** Untreated cells, **b** Cells treated with ZnO NPs synthesized with chemical wet method

(ZnNPs), **c** Cells treated with the only extract, **d** Cells treated with ZnO NPs synthesized from leaf extract (L2-NPs). The bar diagram shows the percentage distributions of the cell cycle

techniques. Moreover, the as-synthesized rod-shaped NPs have been analyzed for anticancer activity against human lung cancer cell lines (A549). The L2-NPs showed 50% cell viability (IC_{50}) at 130.95 $\mu\text{g}/\text{mL}$ for 48 h incubation. The cell viability has been studied by MTT assay, where the results demonstrated that the only extract (OE) and synthesized ZnO NPs with extract of neem leaves (L2-NPs) show apoptosis in cancerous cells by chromatin condensation, cell shrinkage, nuclear, or cytoplasmic fragmentations in the cells, which is further proved by crystal violet assay and AO & PI staining process. ZnO NPs synthesized with the chemical wet method (ZnNPs) have not induced any apoptosis in cancer cells. Both L2-NPs and only extract (OE) treatment in A549 cells have arrested cell cycle in G1 phase, S phase, and G2 phase. But the G1 phase cell percentage has been found higher (i.e., 83.1%) when treated with rod-shaped L2-NPs than treated with the OE of leaves of *Azadirachta indica* (i.e., 79.0%). The neem leaves extract also showed apoptosis by chromatin condensation, cell shrinkage, nuclear, or cytoplasmic fragmentations in A549 lung cancer cells. Our results revealed that advanced experimental research on lung cancer cells must be considered for the determination of universal mechanisms in the anticancer activity of rod-shaped ZnO NPs.

Acknowledgements The authors wish to thank Principal, Miranda House, University of Delhi for providing a lab facility to carry out this research work. D. M. would like to thank the University of Petroleum and Energy Studies (UPES) for providing all the supports. The authors wish to thank the University Scientific Instrumentation Center (USIC), University of Delhi, India for providing SEM, EDS, and PXRD facilities. We also deeply acknowledge to Department of Biotechnology (DBT), New Delhi, India for providing funds under the INDO-US FOLDSCOPE scheme (Sanction order No. BT/IN/Indo/Foldscope/39/2015 dated: 20.03.2018). Recently, our research article has been published on In Vitro study of green synthesized ZnO nanoparticles on human lung cancer cell lines. We have synthesized ZnO NPs with 1, 2, 5, and 10 mL of leaf extract of *Azadirachta indica* (Neem tree). Published data in Materials Today Proceedings are related to ZnO NPs synthesized with 1 mL of leaf extract of *Azadirachta indica*. We have performed the anticancer activity of these synthesized ZnO NPs on the same lung cancer cell lines (A549). Our plan of research is to investigate how the synthesized ZnO with different amounts of leaf extract affects the anticancer activity (IC_{50} value). IC_{50} value for lung cancer cell lines with ZnO NPs synthesized with 1 mL of leaf extract of *Azadirachta indica* (L1-NPs) is found to be 138.50 $\mu\text{g}/\text{mL}$ after 48 h incubation. Whereas, IC_{50} value for L2-NPs is found to be 130.95 $\mu\text{g}/\text{mL}$ after 48 h incubation. We have unpublished data regarding ZnO NPs synthesized with 5 and 10 mL leaf extract. We have taken the same set of parameters of study on the same cancer cell line for comparison purposes. So, already published data and sent data for publication are not the same (as mentioned in Sect. 3.5 & 3.7).

Declarations

Conflicts of interest The authors report no conflicts of interest in this work.

References

- Ahamed M, Khan MAM, Akhtar MJ, Alhadlaq HA, Alshamsan A (2017) Ag-doping regulates the cytotoxicity of TiO_2 nanoparticles via oxidative stress in human cancer cells. *Sci Rep* 7(1):1–14. <https://doi.org/10.1038/s41598-017-17559-9>
- Ahamed M, Akhtar MJ, Khan MAM, Alhadlaq HA (2021) “SnO₂-Doped ZnO/reduced graphene oxide nanocomposites: synthesis, characterization, and improved anticancer activity via oxidative stress pathway. *Int J Nanomed* 16:89–104. <https://doi.org/10.2147/IJN.S285392>
- Akhtar MJ, Ahamed M, Kumar S, Khan MM, Ahmad J, Alkokayan SA (2012) Zinc Oxide nanoparticles selectively induce apoptosis in human cancer cells through reactive oxygen species. *Int J Nanomed* 7:845–857. <https://doi.org/10.2147/IJN.S29129>
- Bharathi D, Bhuvaneshwari V (2019) Synthesis of zinc oxide nanoparticles (ZnO NPs) using pure bioflavonoid rutin and their biomedical applications: antibacterial, antioxidant and cytotoxic activities. *Res Chem Intermed* 45:2065–2078. <https://doi.org/10.1007/s11164-018-03717-9>
- Cheng J, Wang X, Qiu L, Li Y, Marraiki N, Elgorban AM, Xue L (2020) Green synthesized zinc oxide nanoparticles regulates the apoptotic expression in bone cancer cells MG-63 cells. *J Photochem Photobiol B Biol* 202:111644. <https://doi.org/10.1016/j.jphotobiol.2019.111644>
- Govarthanan M, Srinivasan P, Selvakumar T, Janaki V, Al-Misned FA, El-Serehy HA, Kim W, Kamala-Kannan S (2020) Utilization of funnel-shaped ivory flowers of *Candelabra cactus* for zinc oxide nanoparticles synthesis and their in-vitro anti-cancer and antibacterial activity. *Mater Lett* 273:127951. <https://doi.org/10.1016/j.matlet.2020.127951>
- Guo D, Wu C, Jiang H, Li Q, Wang X, Chen B (2008) Synergistic cytotoxic effect of different sized ZnO nanoparticles and daunorubicin against leukemia cancer cells under UV irradiation. *J Photochem Photobiol B* 93:119–126. <https://doi.org/10.1016/j.jphotobiol.2008.07.009>
- Haitao Z, Liang Z, Zhang J, Wang W, Zhang H, Lu Q (2020) Zinc oxide nanoparticle synthesized from *Euphorbia fischeriana* root inhibits the cancer cell growth through modulation of apoptotic signaling pathways in lung cancer cells. *Arab J Chem* 13(7):6174–6183. <https://doi.org/10.1016/j.arabjc.2020.05.020>
- Hamrouni A, Moussa N, Parrino F, Di Paola A, Houas A, Palmisano L (2014) Sol-gel synthesis and photocatalytic activity of ZnO-SnO₂ nanocomposites. *J Mol Catal Chem*. 390:133–141. <https://doi.org/10.1016/j.molcata.2014.03.018>
- Hanley C, Layne J, Punnoose A, Reddy KM, Coombs I, Coombs A (2008) Preferential killing of cancer cells and activated human T cells using ZnO nanoparticles. *Nanotechnology* 19(29):295103. <https://doi.org/10.1088/0957-4484/19/29/295103>
- Jayaseelan C, Abdul Rahumana A, Vishnu Kirthi A, Marimuthua S, Santhoshkumar T, Bagavana A, Gaurav K, Karthik L, Bhaskara Rao KV (2012) Novel microbial route to synthesize ZnO nanoparticles using *Aeromonas hydrophila* and their activity against pathogenic bacteria and fungi. *Spectrochim Acta A Mol Biomol Spectrosc* 90:78–84
- Khan MAM, Kumar S, Alhazaa AN, Al-Gawati MA (2018) Modifications in structural, morphological, optical and photocatalytic properties of ZnO: Mn nanoparticles by sol-gel protocol. *Mater Sci Semicond Proc* 87:134–141. <https://doi.org/10.1016/j.mssp.2018.07.016>
- Kumar S, Suresh PK, Vijayababu MR, Arunkumar A, Arunakaran J (2006) Anticancer effects of ethanolic neem leaf extract on

- prostate cancer cell line (PC3). *J Ethnopharmacol* 105:246–250. <https://doi.org/10.1016/j.jep.2005.11.006>
- Li J, Guo D, Wang X, Wang H, Jiang H, Chen B (2010) The Photodynamic effect of different size ZnO nanoparticles on cancer cell proliferation in vitro. *Nanoscale Res Lett* 5:1063–1071. <https://doi.org/10.1007/s11671-010-9603-4>
- Mahdizadeh R, Tabrizi MH, Neamati A, Seyedi SMR, Afshar HST (2019) Green synthesized-zinc oxide nanoparticles, the strong apoptosis inducer as an exclusive antitumor agent in murine breast tumor model and human breast cancer cell lines (MCF7). *J Cell Biochem* 10:1–10. <https://doi.org/10.1002/jcb.29065>
- Martínez-Carmona M, Gunko Y, Vallet-Regí M, ZnO M (2018) Nanostructures for drug delivery and theranostic applications. *Nanomaterials* 8:268. <https://doi.org/10.3390/nano8040268>
- Mishra PK, Mishra H, Ekielski A, Talegaonkar S, Vaidya B (2017) Zinc oxide nanoparticles: a promising nanomaterial for biomedical applications. *Drug Discov Today* 22(12):1825–1834. <https://doi.org/10.1016/j.drudis.2017.08.006>
- Mohamed Asik R, Gowdhami B, Mohamed Jaabir MS, Archunan G, Suganthi N (2019) Anticancer potential of zinc oxide nanoparticles against cervical carcinoma cells synthesized via biogenic route using aqueous extract of *Gracilaria edulis*. *Mater Sci Eng C* 103:109840. <https://doi.org/10.1016/j.msec.2019.109840>
- Moharram AH, Mansour SA, Hussein MA, Rashad M (2014) Direct Precipitation and characterization of ZnO Nanoparticles. *J Nanomater*. <https://doi.org/10.1155/2014/716210>
- Ostrovsky S, Kazimirsky G, Gedanken A, Brodie C (2009) Selective cytotoxic effect of ZnO nanoparticles on glioma cells. *Nano Res* 2:882–890. <https://doi.org/10.1007/s12274-009-9089-5>
- Padalia H, Chanda S (2017) Characterization, antifungal and cytotoxic evaluation of green synthesized zinc oxide nanoparticles using *Ziziphus nummularia* leaf extract. *Artif Cells Nanomed Biotechnol* 45(8):1751–1761. <https://doi.org/10.1080/21691401.2017.1282868>
- Prashanth GK, Prashanth PA, Bora U, Gadewar M, Nagabhushana BM, Ananda S, Krishnaiah GM, Sathyananda HM (2015) In vitro antibacterial and cytotoxicity studies of ZnO nanoparticles prepared by combustion assisted facile green synthesis. *Karbala Int J Modern Sci* 1(2):67–77. <https://doi.org/10.1016/j.kijoms.2015.10.007>
- Rahimi Kalateh Shah Mohammad G, Karimi E, Oskoueian E, Homayouni-Tabrizi M (2020) Anticancer properties of green-synthesized zinc oxide nanoparticles using *Hyssopus officinalis* extract on prostate carcinoma cells and its effects on testicular damage and spermatogenesis in Balb/C mice. *Andrologia* 52:e13450. <https://doi.org/10.1111/and.13450>
- RahimiKalatehShahMohammad G, Seyedi SMR, Karimi E, Homayouni-Tabrizi M (2019) The cytotoxic properties of zinc oxide nanoparticles on the rat liver and spleen, and its anticancer impacts on human liver cancer cell lines. *J Biochem Mol Toxicol* 33(7):e22324. <https://doi.org/10.1002/jbt.22324>
- Rajeshkumar S, Kumar SV, Ramaiah A, Agarwal H, Lakshmi T, Roopan SM (2018) Biosynthesis of zinc oxide nanoparticles using *Mangifera indica* leaves and evaluation of their antioxidant and cytotoxic properties in lung cancer (A549) cells. *Enzyme Microb Technol* 117:91–95. <https://doi.org/10.1016/j.enzmictec.2018.06.009>
- Ramesh M, Anbuvaran M, Viruthagiri G (2015) Green synthesis of ZnO nanoparticles using *Solanum nigrum* leaf extract and their antibacterial activity. *Spectrochim Acta A Mol Biomol Spectrosc* 136:864–870. <https://doi.org/10.1016/j.saa.2014.09.105>
- Rani N, Saini M, Yadav S, Gupta K, Saini K, Khanuja M (2020) High performance super-capacitor based on rod shaped nanostructure electrode. *AIP Conf Proc* 2276:020042. <https://doi.org/10.1063/5.0026084>
- Rasmussen JW, Martinez E, Louka P, Wingett DG (2010) Zinc oxide nanoparticles for selective destruction of tumor cells and potential for drug delivery applications. *Expert Opin Drug Deliv* 7:1063–1077. <https://doi.org/10.1517/17425247.2010.502560>
- Rauf MA, Oves M, Rehman FU, Khan AR, Husain N (2019) Bougainvillea flower extract mediated zinc oxide's nanomaterials for antimicrobial and anticancer activity. *Biomed Pharmacother* 116:108983. <https://doi.org/10.1016/j.biopha.2019.108983>
- Rozzak J, Catalán J, Järventaus H, Lindberg HK, Suhonen S, Vip-pola M, Stepnik M, Norppa H (2016) Effect of particle size and dispersion status on cytotoxicity and genotoxicity of zinc oxide in human bronchial epithelial cells. *Mutat Res Genet Toxicol Environ Mutagen* 805:7–18. <https://doi.org/10.1016/j.mrgentox.2016.05.008>
- Ryter SW, Kim HP, Hoetzel A, Park JW, Nakahira K, Wang X, Choi AM (2007) Mechanisms of cell death in oxidative stress. *Antioxid Redox Signal* 9(1):49–89. <https://doi.org/10.1089/ars.2007.9.49>
- Salari S, Neamati A, Tabrizi MH, Seyedi SMR (2019) Green synthesized Zinc oxide nanoparticle, an efficient safe anticancer compound for human breast MCF-7 cancer cells. *Appl Organomet Chem* 34(6):e5417. <https://doi.org/10.1002/aoc.5417>
- Salari S, Neamati A, Tabrizi MH, Seyedi SMR (2020) Green-synthesized Zinc oxide nanoparticle, an efficient safe anticancer compound for human breast MCF7 cancer cells. *Appl Organomet Chem* 34(3):e5417. <https://doi.org/10.1002/aoc.5417>
- Selim YA, Azb MA, Ragab I, Abd El-Azim MHM (2020a) Green synthesis of zinc oxide nanoparticles using aqueous extract of *Deverra tortuosa* and their cytotoxic activities. *Sci Rep* 10:3445. <https://doi.org/10.1038/s41598-020-60541-1>
- Selim YA, Azb MA, Ragab I, Abd El-Azim MH (2020b) Green synthesis of zinc oxide nanoparticles using aqueous extract of *Deverra tortuosa* and their cytotoxic activities. *Sci Rep* 10(1):3445. <https://doi.org/10.1038/s41598-020-60541-1>
- Seo H-K, Shin H-S (2015) Study on the photocatalytic activity of ZnO nanodisks for the degradation of Rhodamine B dye. *Mater Lett* 159:265–268. <https://doi.org/10.1016/j.matlet.2015.06.094>
- Sharma V, Anderson D, Dhawan A (2012) Zinc oxide nanoparticles induce oxidative DNA damage and ROS-triggered mitochondria mediated apoptosis in human liver cells (HepG2). *Apoptosis* 17:852–870. <https://doi.org/10.1007/s10495-012-0705-6>
- Sharmila G, Thirumarimurugan M, Muthukumaran C (2019) Green synthesis of ZnO nanoparticles using *Tecoma castanifolia* leaf extract Characterization and evaluation of its antioxidant, bactericidal and anticancer activities. *Microc* 145:578–587. <https://doi.org/10.1016/j.microc.2018.11.022>
- Shilpa VP, Samuel Thavamani B, Roshni ER, Sangeetha Vijayan U, Lekshmi MS, Panicker S, Bhagyasree G, Jilsha KM (2020) Green synthesis of zinc oxide nanoparticles nanoparticle using *Allamanda cathartica* leaf extract and their cytotoxic and antibacterial activity. *Nanomed Res J* 5(3):298–305
- Sisubalan N, Ramkumar VS, Pugazhendhi A, Karthikeyan C, Indira K, Gopinath K, Hameed ASH, Basha MHG (2017) ROS-mediated cytotoxic activity of ZnO and CeO₂ nanoparticles synthesized using the *Rubia cordifolia* L. leaf extract on MG-63 human osteosarcoma cell lines. *Environ Sci Pollut Res Int* 25(11):10482–10492. <https://doi.org/10.1007/s11356-017-0003-5>
- Sivaraj R, Pattanathu Rahman KSM, Rajiv P, Venkatesh R (2014) Biogenic zinc oxide nanoparticles synthesis using *tabernaemontana divaricate* leaf extract and its anticancer activity against MCF-7 breast cancer cell lines. In: International Conference on Advances in Agricultural, Biological & Environmental Sciences (AABES-2014) Oct 15–16, 2014 Dubai (UAE) <https://doi.org/10.15242/IICBE.C1014032>
- Song W, Zhang J, Guo J, Zhang J, Ding F, Li L, Sun Z (2010) Role of the dissolved zinc ion and reactive oxygen species in cytotoxicity

- of ZnO nanoparticles. *Toxicol Lett* 199:389–397. <https://doi.org/10.1016/j.toxlet.2010.10.003>
- Soto-Robles CA, Luque PA, Gomez-Gutierrez CM, Nava O, Vilchis-Nestor AR, Lugo-Medina E, Ranjithkumar R, Castro-Beltran A (2019) Study on the effect of the concentration of *Hibiscus sabdariffa* extract on the green synthesis of ZnO nanoparticles. *Res Phys* 15:102807. <https://doi.org/10.1016/j.rinp.2019.102807>
- Stowe DF, Camara AKS (2009) Mitochondrial reactive oxygen species production in excitable cells: modulators of mitochondrial and cell function. *Antioxid Redox Signal* 11:1373–1414. <https://doi.org/10.1089/ars.2008.2331>
- Sukri SNAM, Shameli K, Wong MMT, Teow SY, Chew J, Ismail NA (2019) Cytotoxicity and antibacterial activities of plant-mediated synthesized zinc oxide (ZnO) nanoparticles using *Punica granatum* (pomegranate) fruit peels extract. *J Mol Struct* 1189:57–65. <https://doi.org/10.1016/j.molstruc.2019.04.026>
- Suresh J, Pradheesh G, Alexamani V, Sundrarajan M, Hong SI (2018) Green synthesis and characterization of zinc oxide nanoparticle using insulin plant (*Costus pictus* D Don) and investigation of its antimicrobial as well as anticancer activities. *Adv Nat Sci Nanosci Nanotechnol* 9(1):015008
- Tanino R, Amano Y, Tong X (2020) Anticancer activity of ZnO nanoparticles against human small-cell lung cancer in an orthotopic mouse model. *Mol Cancer Ther* 19(2):502–512. <https://doi.org/10.1158/1535-7163>
- Umamaheswari A, Lakshmana Prabu S, Adharsh John S, Puratchikody A (2021) Green synthesis of zinc oxide nanoparticles using leaf extracts of *Raphanus sativus* var. *Longipinnatus* and evaluation of their anticancer property in A549 cell lines. *Biotechnol Rep* 29:e00595. <https://doi.org/10.1016/j.btre.2021.e00595>
- Wahab R, Siddiqui MA, Saquib Q, Dwivedi S, Ahmad J, Mussarat J, Al-Khedhairi AA, Shin HS (2014) ZnO Nanoparticles induced oxidative stress and apoptosis in HepG2 and MCF-7 Cancer cells and their antibacterial activity. *Colloids Surf B* 117:267–276. <https://doi.org/10.1016/j.colsurfb.2014.02.038>
- Wang M, Thanou M (2010) Targeting nanoparticles to cancer. *Pharmacol Res* 62(2):90–99. <https://doi.org/10.1016/j.phrs.2010.03.005>
- Wang C, Hu X, Gao Y, Ji Y (2015) ZnO nanoparticles treatment induces apoptosis by increasing intracellular ROS Levels in LTP-a-2 Cells. *BioMed Res Int*. <https://doi.org/10.1155/2015/423287>
- Xiong HM (2013) ZnO nanoparticles applied to bioimaging and drug delivery. *Adv Mater* 25:5329–5335. <https://doi.org/10.1002/adma.201301732>
- Zhang H, Pokhrel S, Ji Z, Meng H, Wang X, Lin S, Chang CH, Li L, Li R, Sun B, Wang M, Liao YP, Liu R, Xia T, Madler L, Nel AE (2014) PdO doping tunes band-gap energy levels as well as oxidative stress responses to a Co_3O_4 p-type semiconductor in cells and the lung. *J Am Chem Soc* 136(17):6406–6420. <https://doi.org/10.1021/ja501699e>

Publisher's Note Springer Nature remains neutral with regard to jurisdictional claims in published maps and institutional affiliations.

Authors and Affiliations

Nutan Rani¹ · Kavita Rawat² · Mona Saini¹ · Anju Shrivastava² · Ganeshlenin Kandasamy³ · Kalawati Saini¹ · Dipak Maity⁴ 

¹ Department of Chemistry, Miranda House, University of Delhi, Patel Chest Marg, New Delhi 110007, India

² Department of Zoology, University of Delhi, North Campus, New Delhi 110007, India

³ Department of Biomedical Engineering, Vel Tech Rangarajan Dr. Sagunthala R&D Institute of Science and Technology, Chennai, Tamil Nadu, India

⁴ Department of Chemical Engineering, University of Petroleum and Energy Studies, Dehradun, India